



Athanasia Proklou<sup>1,2</sup>, Maria Bolaki<sup>1</sup>, Evangelia E. Vassalou<sup>3</sup>,  
Eleni Bibaki<sup>1</sup>, Eirini Vasarmidi<sup>1</sup>, George A. Margaritopoulos<sup>4</sup>,  
Apostolos H. Karantanas<sup>1,3</sup>, Nikolaos Tzanakis<sup>1</sup>, Katerina M. Antoniou<sup>1</sup>



kantoniou@uoc.gr



<sup>1</sup>Dept of Thoracic Medicine, Heraklion University Hospital, Medical School, University of Crete, Heraklion, Greece. <sup>2</sup>ICU, Heraklion University Hospital, Medical School, University of Crete, Heraklion, Greece. <sup>3</sup>Dept of Medical Imaging, Heraklion University Hospital, Medical School, University of Crete, Heraklion, Greece. <sup>4</sup>ILD Unit, Royal Brompton Hospital, London, UK.

# Paroxysmal cough and left sacroiliac joint pain in a 50-year-old Caucasian man

## Case report

A 50-year-old Caucasian man who was a lifelong nonsmoker presented with a 3-year history of paroxysmal dry cough, fatigue, nonspecific myalgias, muscle weakness of the lower extremities and left sacroiliac joint pain. Initially, he was reviewed by a pulmonologist and subsequently he was referred to the Dept of Thoracic Medicine (Heraklion University Hospital, Heraklion, Greece) for further investigation. His medical history was remarkable for the presence of arterial hypertension on treatment with amlodipine and irbesartan.

A full blood cell count showed a white blood cell count of  $5.6 \times 10^3$  cells· $\mu\text{L}^{-1}$ , with a lymphocyte count of  $2.0 \times 10^3$  cells· $\mu\text{L}^{-1}$  (35%). Lactate dehydrogenase (LDH) and angiotensin-converting enzyme (ACE) were increased to  $440 \text{ U}\cdot\text{L}^{-1}$  (normal range  $90\text{--}250 \text{ U}\cdot\text{L}^{-1}$ ) and  $105.5 \text{ U}\cdot\text{L}^{-1}$  (normal range  $8\text{--}52 \text{ U}\cdot\text{L}^{-1}$ ), respectively. The autoantibody profile

and the inflammatory markers were unremarkable. Additionally, a 24-h urine collection revealed increased calcium concentration (355 mg; normal range 80–300 mg). Creatine kinase, serum calcium and alkaline phosphatase levels were measured within normal limits.

Lung function testing showed a mixed pattern, with a forced expiratory volume in 1 s (FEV<sub>1</sub>) of 2.73 L (74.7% predicted), forced vital capacity (FVC) of 3.83 L (84.6% pred), ratio of FEV<sub>1</sub>/FVC of 71.35%, total lung capacity of 77% pred and single-breath diffusing capacity of the lung for carbon monoxide, corrected for haemoglobin concentration, of 93% pred.

An ECG revealed a right bundle branch block (RBBB) without other abnormalities. Chest radiography showed left hilar enlargement as well as ill-defined reticulonodular opacities in the left middle lung field.

**Cite as:** Proklou A, Bolaki M, Vassalou EE, *et al.* Paroxysmal cough and left sacroiliac joint pain in a 50-year-old Caucasian man. *Breathe* 2018; 14: e59–e67.

### Task 1

What would be your next investigation in this patient, to better define the thoracic abnormalities?



@ERSpublications

Can you diagnose this patient with pulmonary symptoms, thoracic and laboratory test abnormalities and sacroiliac joint pain? <http://ow.ly/LPyy30kaViz>



© ERS 2018

**Answer 1**

High-resolution computed tomography (CT) of the chest, in order to investigate both the mediastinum and lung parenchyma lesions.

Due to the thoracic abnormalities we conducted a chest CT, which revealed mildly enlarged paratracheal, aortopulmonary and hilar lymph

nodes. Some of them contained amorphous or eggshell calcifications (figure 1a). Nodules with a distribution along the peribronchovascular bundles with upper and middle zone predominance were observed. A few subpleural nodules could also be noted (figure 1b). There were some nodules with irregular margins, measuring up to 1 cm, distributed through the upper and middle lung fields.

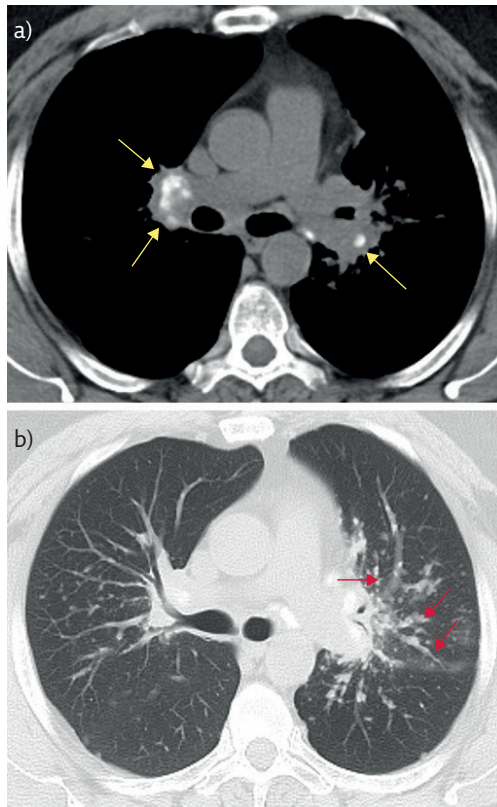


**Figure 1** a) CT axial image in a mediastinal window shows bilateral enlarged hilar lymph nodes containing amorphous calcifications (arrows). b) CT image in a lung window at the level of middle lung fields demonstrates micronodular thickening of the bronchovascular sheaths extending to the lung periphery (arrows).

**Task 2**

What could be the differential diagnoses, in the light of the clinical presentation and imaging results?

**Answer 2**

The differential diagnoses include pulmonary sarcoidosis, metastatic disease and atypical infection.

A subsequent flexible bronchoscopy showed narrowing of the left upper and lingular bronchus. Endobronchial biopsy revealed non-caseating granulomas and bronchoalveolar lavage fluid analysis showed 88.4% macrophages, 7.4%

lymphocytes and 2.4% epithelial cells. Special stains and culture for bacteria, mycobacteria and fungus tested negative. The CD4/CD8 ratio was 1.55.

Furthermore, we investigated the potential central nervous system involvement. An electroencephalogram was performed, with unremarkable findings. An electromyogram evaluation indicated no myogenic changes, and ophthalmological assessment with fluorescence angiography was negative for microvascular ocular involvement.

**Task 3**

What would be your next step in order to interpret the ECG abnormalities and the chronic left sacroiliac joint pain?

**Answer 3**  
Cardiac magnetic resonance imaging (MRI)  
and pelvic MRI, respectively.

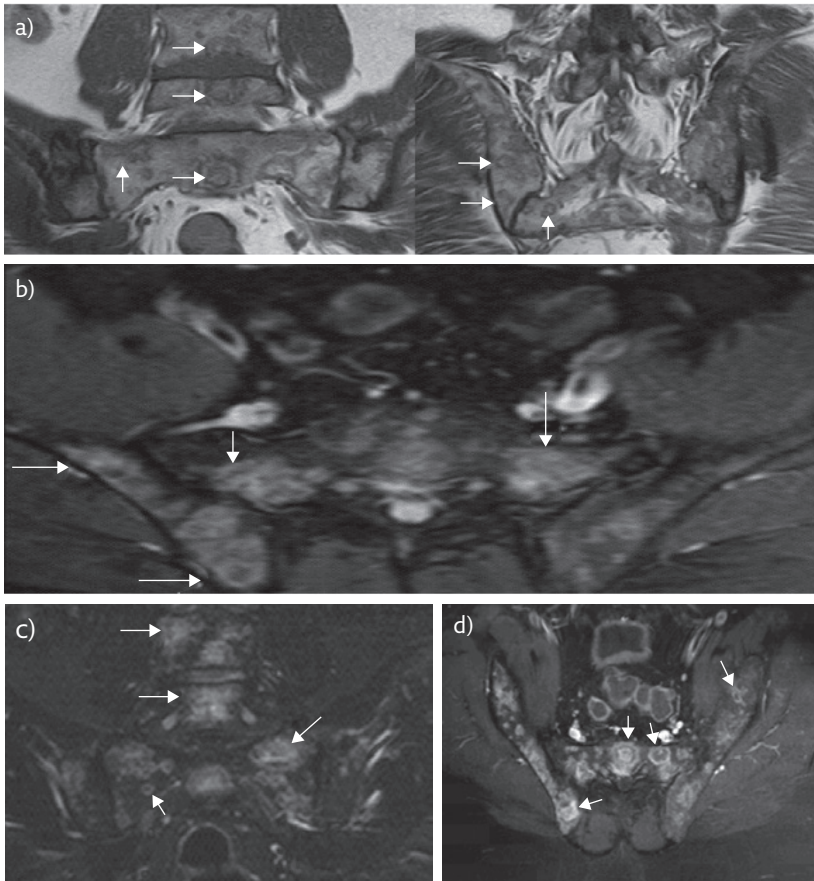


**Figure 2** MRI. a) Oblique coronal and axial T1w MRI shows multiple lesions in L4, L5, sacrum and iliac bones exhibiting a ring or double rings of low signal intensity with fatty element in the central part (arrows). b) Axial and c) oblique coronal STIR MRI shows the multiple lesions exhibiting high signal intensity (arrows). A reversed pattern as opposed to the T1w images is seen in some lesions. d) Axial fat-suppressed contrast-enhanced MRI shows to better advantage the ring enhancement pattern and in some lesions the additional central enhancement (arrows).

Given the RBBB in the absence of ischaemic heart disease, we performed cardiac MRI, which demonstrated signs of inflammation and fibrosis in

the interventricular septum, suggestive of cardiac sarcoidosis. Holter evaluation did not show any ventricular arrhythmias.

We performed whole-body  $^{18}\text{F}$ -fluorodeoxyglucose ( $^{18}\text{F}$ -FDG) positron emission tomography/CT, which showed increased  $^{18}\text{F}$ -FDG uptake at the site of the previous surgical intervention biopsy path at the right iliac crest, as well as calcified mediastinal, hilar and upper abdominal lymph nodes, and a few pulmonary nodules with inflammatory characteristics. These findings were described as signs of chronic granulomatous disease, with no signs of active cardiac involvement.

Due to persistent left sacroiliac joint pain, we performed pelvic MRI, which revealed innumerable, variably sized, intramedullary lesions finely distributed through the lower lumbar vertebrae, sacrum, iliac, pubic and ischial bones, as well as proximal femoral metaphysis (figure 2a). A limited extraosseous soft tissue component with intraspinal extension was evident at the level of the S2 vertebral body. Involvement of the posterior elements was present at the L5–S2 levels. Most lesions showed a sharply defined, serpiginous border on all pulse sequences while a minority of them, especially those located on the left iliac bone, exhibited a border interdigitating with surrounding fatty bone marrow. The majority of the lesions demonstrated a target appearance with concentric hyperintense (inner) and hypointense (outer) rings surrounding a central area of intermediate signal intensity on T1w images. A reversed pattern was observed on short tau inversion recovery (STIR) sequences (figure 2b and c). Central foci and/or perilesional areas of T1 shortening, corresponding to areas of low signal intensity on STIR images, characterised the vast majority of the lesions. Small lesions, measuring up to several millimetres, depicted iso- or slight hyperintensity to muscles on T1w images and moderate hyperintensity on fluid-sensitive sequences. Following contrast administration, the pattern of lesional enhancement mostly resembled the signal intensity pattern on STIR sequences (figure 2d), while diffuse enhancement was observed in many, especially smaller, lesions. Differential diagnosis included osseous sarcoidosis and metastatic disease.

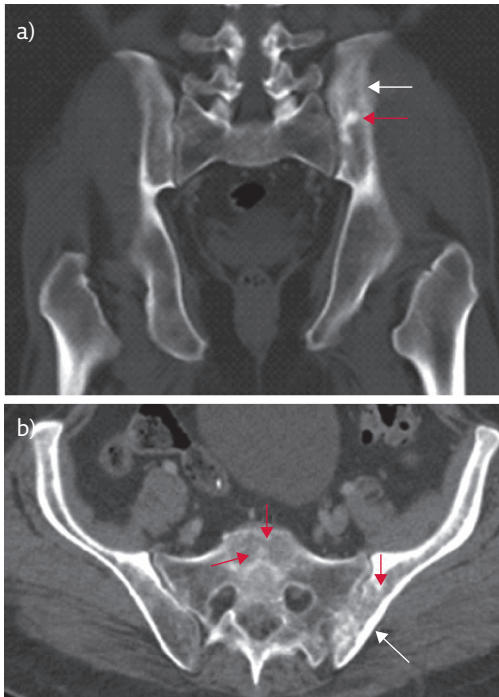


**Figure 3** CT. a) Axial and b) coronal images show a few sclerotic marrow lesions in the bone marrow (red arrows) and generalised osteosclerosis primarily seen in the left iliac bone (white arrows).

In order to exclude a primary malignancy, CT of the abdomen was performed, with unremarkable findings. Faint bone marrow inhomogeneity of the left iliac bone and ipsilateral sacral wing was detected, with interposed sclerotic foci (figure 3).

#### Task 4

Are there any other tests you would perform in order to better characterise these osseous lesions?

**Answer 4**

Biopsy of the osseous lesions in order to exclude malignancy, and full body scintigraphy to investigate further lesions in other parts of the body.

Our major dilemma in the differential diagnosis of this patient was to exclude neoplasia with osseous primary or metastatic origin. In an attempt

to characterise the osseous lesions, in order to exclude neoplastic disease, a bone marrow biopsy was conducted, which had nonspecific findings. Subsequently, the patient underwent an open bone biopsy, which was negative for malignant disease. During further diagnostic work-up, the patient underwent a full body scintigraphy with <sup>67</sup>Ga, which indicated abnormal uptake in the region of the left sacroiliac joint, due to inflammatory disease such as sarcoidosis.

**Task 5**

Given this organ impairment, would you initiate treatment in this patient?

**Answer 5**

Because of the increased calcium concentration in the urine, the cardiac activity and the symptomatic osseous lesions, prednisolone therapy ( $30 \text{ mg}\cdot\text{day}^{-1}$ ) was initiated.

Oral steroid treatment was tapered down to  $20 \text{ mg}\cdot\text{day}^{-1}$  after 6 weeks and finally to  $10 \text{ mg}\cdot\text{day}^{-1}$  in following months. At 5 months after steroid treatment, follow-up pelvic MRI showed complete resolution of the osseous lesions and revealed findings typical of bilateral femoral head avascular necrosis (figure 4), attributed to the history of steroid administration. There was no bone marrow oedema or subchondral fracture. A follow-up CT scan of the thorax at 7 months showed remarkable improvement, with both marked improvement of the peribronchovascular thickening as well as shrinkage of the majority of parenchymal nodules. Mediastinal lymph node calcification was evident. Follow-up cardiac echocardiography did not show any evidence of cardiac dysfunction.

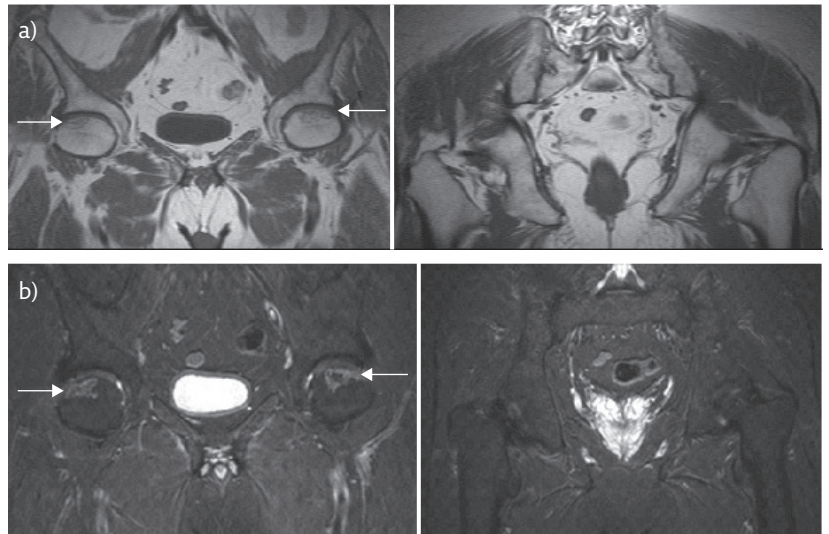


**Figure 4** a) Coronal T1w and b) STIR MRI shows avascular necrosis in the anterior subarticular femoral head bilaterally (arrows) and complete resolution of the old lesions.

**Task 6**

What would be your working diagnosis in the light of the imaging results as well as taking into consideration the initial laboratory results (increased serum LDH and ACE levels and increased calcium concentration in the urine)?

**Answer 6**

The imaging and laboratory findings support the diagnosis of sarcoidosis with pulmonary, cardiac and osseous involvement.

In view of the hypercalciuria, osseous involvement and long-term steroid treatment, we checked the levels of calcium in the blood and urine, plus serum vitamin D levels, every 3 months for a year. They were within the normal range.

The patient remained under low prednisolone dose for 9 months and after the cessation of the drug remains without relapse of the initial bone lesion with an excellent performance status.

**Discussion**

Sarcoidosis is a chronic, multisystemic disease of unknown aetiology characterised by the progressive formation of non-caseating granulomatous lesions and by heterogeneity of clinical manifestations. Symptoms develop more frequently in the fourth and fifth decades of life [1]. Women are affected more frequently than males, with prevalence estimated at around 19 per 100000 and 16.5 per 100000, respectively [2]. Sarcoidosis mainly affects the lungs (>90%), but other organs such as the lymph nodes, eyes, skin, central nervous system, heart and bones can be involved [3]. Isolated extrapulmonary sarcoidosis occurs in only 10% of patients [4]. The diagnosis of sarcoidosis is frequently challenging, as clinical manifestations and imaging findings are often variable and nonspecific [5]. The diagnosis is established when clinical and radiological findings are supported by histological evidence of non-caseating granulomatous inflammation and other causes of granulomas and local reactions have been reasonably excluded [6].

Granulomatous bone involvement has an overall incidence of 1–13%, which is probably underestimated due to lack of specific symptoms. However, recent data suggest a wide range that varies from 3% to 39% of radiographically evident osseous involvement depending on the imaging modalities used. Pelvic, skull, knee, rib and sternal involvement have been rarely reported, whereas sarcoid lesions of the small bones of

the hands and feet have been more frequently described [7, 8]. The most common pattern of osseous involvement is a “lacelike” osteolysis of the hands and feet, although mixed, sclerotic or purely lytic lesions have also been described [9]. On MRI, the appearance and signal intensity characteristics of sarcoid lesions are usually nonspecific [10]. The presence of lesional or perilesional focal fatty areas, also present in our patient, has also been described; however, this sign is characterised by poor sensitivity as it can also be observed in osseous ischaemia [11, 12]. Osseous sarcoidosis should be suspected in cases of multifocal bone lesions and an established diagnosis of sarcoidosis. Imaging findings of osseous sarcoidosis closely resemble metastatic disease, resulting in a clinical dilemma. However, differentiation from metastatic disease cannot be made based solely on imaging findings [11]. CT-guided biopsy is often not possible because most of the lesions are occult on CT, as in the case presented here. Detection of osseous lesions is crucial, because the clinical assessment of granulomatous load may be modified and this could influence treatment management [13]. Additionally, they can affect quality of life as they may be painful.

In the case presented here, the patient was initially suspected of having sarcoidosis, based on the chest CT findings, the increased serum LDH and ACE levels and the increased calcium concentration in the urine. The presence of multiple pelvic osseous lesions could not exclude metastatic disease and the inability to histologically characterise them yielded a clinical dilemma. Because of the increased calcium concentration in the urine, the cardiac activity and the presence of symptomatic osseous lesions, prednisolone therapy was initiated. Optimal treatment of sarcoidosis with osseous involvement remains unclear. In most reports, corticosteroids have been used as a first-line therapy with a reported long-term efficacy in resolving osseous lesions and correcting hypercalcaemia. However, while corticosteroids improve skeletal symptoms, they are associated with increased risk of osteoporosis, pathological fractures and avascular necrosis, as in our case [14, 15]. In conclusion, this case report is important because there is great need to underline the complexity of sarcoidosis, the concern of differential diagnosis with respect to malignancies and the need for appropriate and effective therapy of multisystemic disease.

**Conflict of interest**

None declared.

**References**

1. Iwai K, Tachibana T, Takemura T, *et al*. Pathological studies on sarcoidosis autopsy. I. Epidemiological features of 320 cases in Japan. *Acta Pathol Jpn* 1993; 43: 372–376.
2. Nunes H, Bouvry D, Soler P, *et al*. Sarcoidosis. *Orphanet J Rare Dis* 2007; 2: 46.
3. Valeyre D, Prasse A, Nunes H, *et al*. Sarcoidosis. *Lancet* 2014; 383: 1155–1167.
4. Gioviale M, Fonnesu C, Soriano A, *et al*. Atypical sarcoidosis: case reports and review of the literature. *Eur Rev Med Pharmacol Sci* 2009; 13: Suppl. 1, 37–44.



5. Hunninghake GW, Costabel U, Ando M, *et al.* ATS/ERS/WASOG statement on sarcoidosis. American Thoracic Society/European Respiratory Society/World Association of Sarcoidosis and other Granulomatous Disorders. *Sarcoidosis Vasc Diffuse Lung Dis* 1999; 16: 149-173.
6. Baughman RP, Culver DA, Judson MA. A concise review of pulmonary sarcoidosis. *Am J Respir Crit Care Med* 2011; 183: 573-581.
7. Kuzyshyn H, Feinstein D, Kolasinski SL, *et al.* Osseous sarcoidosis: a case series. *Rheumatol Int* 2015; 35: 925-933.
8. Bargagli E, Olivieri C, Penza F, *et al.* Rare localizations of bone sarcoidosis: two case reports and review of the literature. *Rheumatol Int* 2011; 31: 1503-1506.
9. Hyzy MD, Kroon HM, Watt I, *et al.* Chronic osseous sarcoidosis. *JBR-BTR* 2007; 90: 194-195.
10. Moore SL, Teirstein AE. Musculoskeletal sarcoidosis: spectrum of appearances at MR imaging. *Radiographics* 2003; 23: 1389-1399.
11. Moore SL, Kransdorf MJ, Schweitzer ME, *et al.* Can sarcoidosis and metastatic bone lesions be reliably differentiated on routine MRI? *AJR Am J Roentgenol* 2012; 198: 1387-1393.
12. Simpfendorfer CS, Ilaslan H, Davies AM, *et al.* Does the presence of focal normal marrow fat signal within a tumor on MRI exclude malignancy? An analysis of 184 histologically proven tumors of the pelvic and appendicular skeleton. *Skeletal Radiol* 2008; 37: 797-804.
13. Wilcox A, Bharadwaj P, Sharma OP. Bone sarcoidosis. *Curr Opin Rheumatol* 2000; 12: 321-330.
14. Torralba KD, Quismorio FP Jr. Sarcoidosis and the rheumatologist. *Curr Opin Rheumatol* 2009; 21: 62-70.
15. Zisman DA, Shorr AF, Lynch JP 3rd. Sarcoidosis involving the musculoskeletal system. *Semin Respir Crit Care Med* 2002; 23: 555-570.